ELECTROMAGNETIC RADIATION FROM INGESTED SOURCES IN THE HUMAN INTESTINE

L. C. Chirwa, P. A. Hammond, S. Roy and D. R. S. Cumming

MST Group, Dept. of Electronics & Electrical Engineering, University of Glasgow, Glasgow G12 8LT, UK

***Abstract*—There is currently considerable work on the development of wireless sensors that can be used in the small intestine. The radiation characteristics of sources in the gastro-intestinal (GI) tract cannot be readily calculated due to the complexity of the human body and its composite tissues, each with different electrical characteristics. This paper presents radiation characteristics for sources in the GI tract that should allow for the optimum design of more efficient telemetry systems. The characteristics are determined using the finite difference time domain method with a realistic antenna model on an established fully segmented human body model. Maximum radiation was found to occur between 450 and 900 MHz and the gut region was found generally to inhibit vertically polarized electric fields more than horizontally polarized fields.**

***Index Terms*— Bio-telemetry, Sensor, Gastro-intestinal tract, Human body, Electromagnetics, Radiation characteristics, Finite difference time domain - FDTD.**

I. INTRODUCTION

The conventional way of internally monitoring and examining the human digestive tract is by means of sensors embedded in flexible cannulae. However due to the nature of the flexible cannulae they can not be used in the small intestine. As a result there is currently considerable work on developing small wireless devices that can be swallowed for examining the small intestine. These devices are in the form of wireless "capsules". The sensors and their associated circuitry and transmitter are encased in "capsules" that are small enough to be swallowed and traverse the entire digestive tract while transmitting their readings to an external receiver.

The properties of human tissue are such that their absorption of electromagnetic waves increases with increasing frequency. It would therefore be expected that radiation from an ingested source would decrease with increasing frequency. This is however not the case. This is because the problem of radiation of ingested sources is similar to that of incident fields on several layers of dielectric medium with different constitutive parameters. In this case there exists at least one optimal frequency when the wave propagates through the different media most effectively. For such problems a conceptually simple method such as the impedance transformation approach [1] is used to arrive at solutions of optimal frequencies with relative ease. The optimal frequencies are dependant on the electrical and physical properties of the media. In the case of the human body the structure and relative positioning of its composite tissues is complex, and in addition the tissues have different electrical parameters, namely conductivity and permittivity, which each have a unique frequency dependence. In addition, the propagating waves in the human body will not be plane waves, and the boundaries between different tissue types are rough. It is therefore apparent that the radiation characteristics of implanted sources are not trivial and can not be readily predicted.

The radiation characteristics are important for the reasons stated above where the radiation characteristics are not readily predictable especially when the radiation efficiency is very low due to the antennas used being electrically small as they have to be resident in the wireless capsules, which have a maximum dimension of only a few centimetres. In addition highly efficient telemetry systems are required in view of these devices being very low power as they are battery operated. It is in this regard that this work determines the radiation characteristics of electromagnetic sources in the small intestine, using the finite difference time domain (FDTD) method [2].

II. THE HUMAN BODY MODEL

A commercial fully established segmented realistic model of a male human subject made up of cubic voxels with an edge size of 5 mm was used [3]. This cell size takes into consideration the computer resources that would be required for a simulation in "good" time on a relatively fast computer (1.5 GHz Pentium IV processor). Each voxel edge in the mesh is defined as one of 25 groups of tissue types. The model was developed from data from the Visible Human Project sponsored by the National Library of Medicine (NLM) [4]. The data in the project is of axial anatomical cross-sections at 1 mm intervals. The entire mesh including buffer cells is $136 \times 87 \times 397$ cells (4,697,304 cells).

III. ANALYSIS

The FDTD method was used as it is a versatile technique appropriate for evaluating electromagnetic fields in complex

structures. The FDTD problem space was terminated by Liao's absorbing boundary condition (ABC) [5]. Liao ABC terminated work spaces take considerably less time to compute than those of equal size terminated by PML [6] ABC, while hardly compromising accuracy.

Though wide band excitation would be the more efficient method (requiring only one run to determine parameters at all frequencies in the excitation band width) for this problem, single fixed frequency sinusoidal excitation was utilized as the source model employed required specific phase relationships between its composite source elements. Simulations were conducted at specific frequencies over a wide frequency spectrum.

A typical capsule device may allow a helical antenna with a maximum dimension of about 8 mm. Clearly the relatively large grid size of 5 mm used here does not allow for the modelling of an antenna of such dimensions in adequate detail to obtain credible results. In addition the one cell (delta gap) excitation is employed. Therefore the size of the feeding gap is comparable to the dimensions of the antenna being modelled, and as a consequence the FDTD calculation results are erroneous. A solution to this is to place the helix in a finer sub grid in which it is modelled accurately. In this case however a finer mesh with grid spacing of 0.5 mm would be required to model the antenna accurately. However this results in the reduction of the Courant time step [2] and a corresponding increase in the total number of time steps (equal to the inverse of the decrease in the Courant time step) required for the simulation. The increase is by a factor of about 17. Even using a 1 mm sub grid that would allow for a reasonable coarse modelling of the antenna used here results in an increase of the simulation time of close to ten times. As a result the model of a normal mode monofilar helix antenna similar to that in [8] was employed. It utilizes a series of equivalent electrical and magnetic sources to produce fields similar to that of a monofilar helix antenna operating in normal mode. This model produces accurate far fields while its near fields may suffer from errors of up to 10 %. In this case the magnetic fields were replaced by their equivalent electric fields, due to the limitations of the simulation tool used [3].

The monofilar helix antenna modelled had a diameter of 8 mm, length of 4 mm and pitch 1 mm. Its free space vertical to horizontal polarization ratio (E_θ/E_ϕ) was 13 dB with an electric field left circular polarization (ELCP) to right circular polarization (ERCP) ratio of about 3.5 dB making the radiated field predominantly linear.

Three orientations, all orthogonal to each other, of the source in the intestines were considered. The orientations are vertical, transverse-horizontal and longitudinally-horizontal and are shown respectively in Figures 1c to 1e.

Extensive simulations were performed for sources at many locations in the small intestine. Here, for brevity, we present results for the three locations shown in Fig. 1 only. These results are however representative of the overall results obtained. Position A is deep-set in the middle of the gut, while B is also deep-set but at the lower limits of the small intestine.

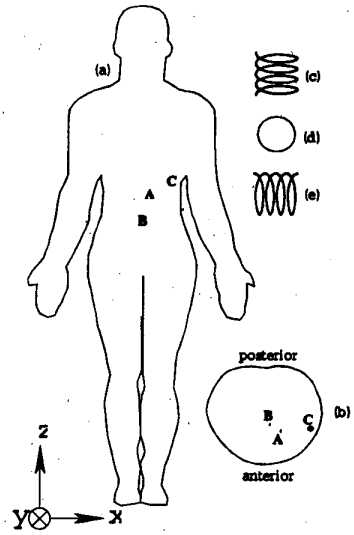

Fig. 1. Location and orientation of ingested sources. (a) Location in the vertical-transverse plane. (b) Location in the axial-transverse plane. (c) Vertical orientation. (d) Transverse-horizontal orientation. (d) longitudinally-horizontal orientation.

C is close to the skin surface on the left side of the body.

IV. Results

Numerous simulations were conducted at specific frequencies over a wide frequency spectrum. From these simulation results it was evident that the radiated electric field intensity was maximum in the 0.15–1.2 GHz range. This range coincidentally covers the frequencies recommended as the pan-European frequency allocations for short range applications [7], and, the US Federal Communications Commission (FCC) frequency allocations for bio-medical telemetry and industrial, scientific and medical (ISM) devices (regulations S5.150, US290 and US350).

The pass band radiation effect can be observed in both the near (Figures 2 to 5) and far (Figures 6 to 9) fields. Figures 2 to 5 are of normalized (normalized by the maximum total electric field for all cases) fields taken in the direction of maximum radiated electric field intensity in the same plane as the radiating source. The power of the radiating source is taken to be the same for all cases. The sampling points are on the exterior of the body at distances of between 1 and 1.5 cm from the body skin surface and are all on the anterior of the body. The electric field components have the directions shown in Fig. 1. Figures 6 to 9 show the corresponding transverse plane far field patterns.

For the source at A the total field comprises mainly of E_x from 150 to 434 MHz, and from 600 MHz to 1 GHz it mainly comprises of E_y. At 1.2 GHz E_x is again dominant. This phenomenon is mirrored in the far fields where E_θ is

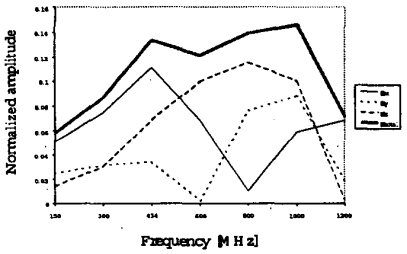

Fig. 2. Near electric field normalized amplitude for ingested transverse-horizontally orientated 434 MHz source at *A*.

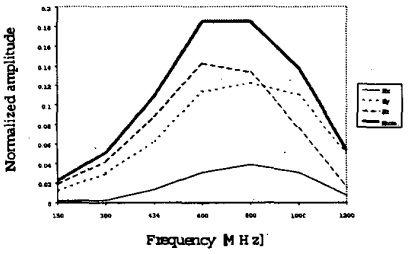

Fig. 3. Near electric field normalized amplitude for ingested vertically orientated 434 MHz source at *B*.

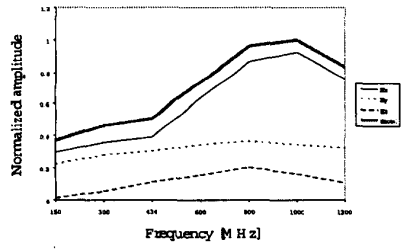

Fig. 4. Near electric field normalized amplitude for ingested transverse-horizontally orientated 434 MHz source at *B*.

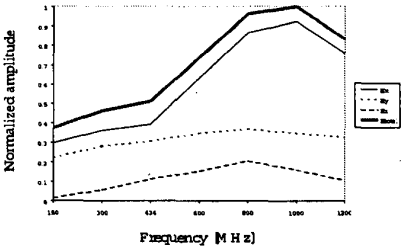

Fig. 5. Near electric field normalized amplitude for ingested transverse-horizontally orientated 434 MHz source at *C*.

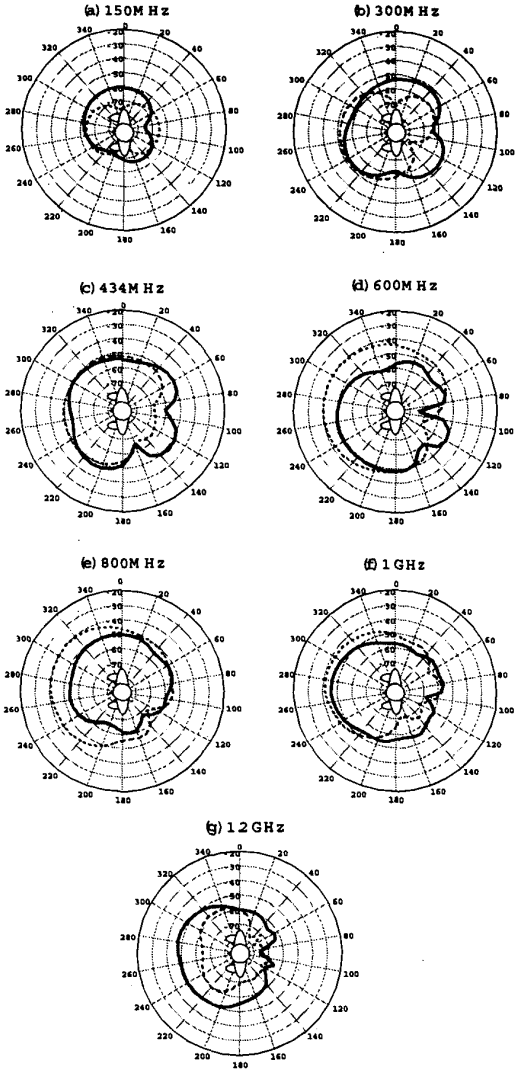

Fig. 6. Azimuthal far fields for transverse-horizontally orientated ingested source at *A*. (a) 150 MHz. (b) 300 MHz. (c) 434 MHz. (d) 600 MHz. (e) 800 MHz. (f) 1 GHz. (g) 1.2 GHz. (dashed line). Vertically polarized pattern. (solid line) Horizontally polarized pattern.

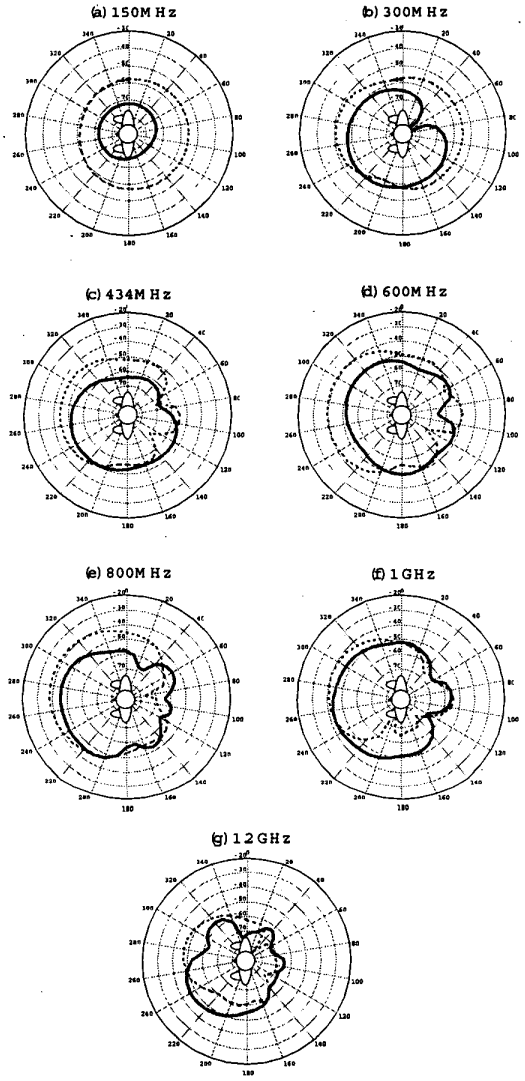

Fig. 7. Azimuthal far fields for vertically orientated ingested source at B. (a) 150 MHz. (b) 300 MHz. (c) 434 MHz. (d) 600 MHz. (e) 800 MHz. (f) 1 GHz. (g) 1.2 GHz. (dashed line). Vertically polarized pattern. (solid line) Horizontally polarized pattern.

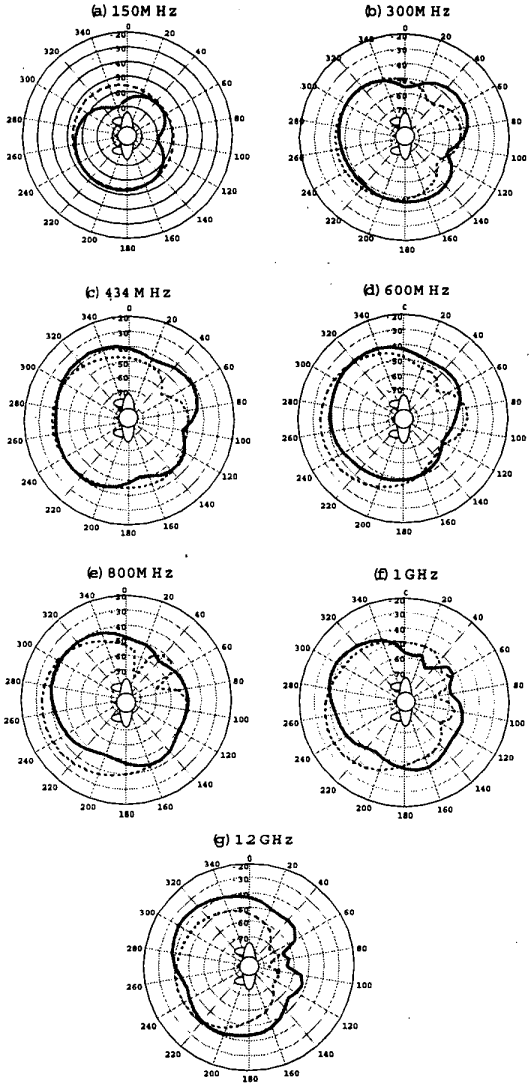

Fig. 8. Azimuthal far fields for transverse-horizontally orientated ingested source at B. (a) 150 MHz. (b) 300 MHz. (c) 434 MHz. (d) 600 MHz. (e) 800 MHz. (f) 1 GHz. (g) 1.2 GHz. (dashed line). Vertically polarized pattern. (solid line) Horizontally polarized pattern.

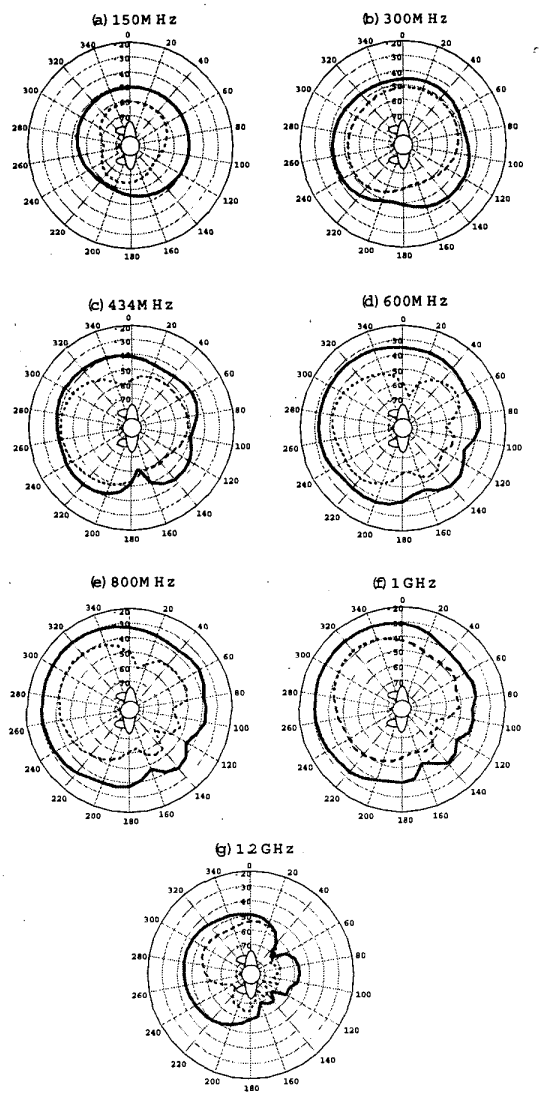

Fig. 9. Azimuthal far fields for transverse-horizontally orientated ingested source at C. (a) 150 MHz. (b) 300 MHz. (c) 434 MHz. (d) 600 MHz. (e) 800 MHz. (f) 1 GHz. (g) 1.2 GHz. (dashed line). Vertically polarized pattern. (solid line) Horizontally polarized pattern.

greater than E_ϕ from 600 MHz to 1 GHz, and at 1.2 GHz E_ϕ is greater than E_θ in the anterior direction. For a vertically oriented source at B the dominant near field is E_y and the dominant far field polarization is E_θ. When the orientation of the source at B changes from vertical to transverse-horizontal both near and far fields reduce in magnitude, indicating that horizontally polarized fields are attenuated more strongly than vertically polarized ones. The optimum frequency for maximum radiation is seen to shift from 800 to 600 MHz.

The findings for sources at B are consistent with the practical measured results in [9] probably because position B is close to the position of the source in [9]. This result infers that the rest of the results are accurate as well.

For the case when the source is near the body skin surface the near fields increase by a factor of more than 3.5 and the far fields increase correspondingly by more than 10 dB. This is expected because of the reduced amount of tissue between the radiating source and body exterior. Regardless of the reduced amount of tissue the external radiation intensity also exhibits a Guassian like relationship with frequency.

V. Conclusion

Both the near and far field radiation from sources in the intestine are always maximum on the anterior side of the body. The results suggest that deep set ingested devices are most efficient in the 450–900 MHz range. Outside this range the fields are greatly attenuated. The maximum far fields occur in the 600 MHz to 1 GHz range. The weakest fields are obtained from deep set sources, and are lower than those from sources near the body skin surface by a factor of over 3.5 for near fields and 10 dB for far fields. Radiated fields from vertically polarized sources are more greatly attenuated than horizontally polarized sources.

These results however only serve as a guide as humans differ significantly in posture, morphology, size and weight.

References

[1] David K. Cheng *Field and Wave Electromagnetics*, Addison-Wesley Publishing Company, 1989.

[2] A. Taflove, *Computational Electrodynamics: The Finite-Difference Time-Domain Method*, Artech House, 1995.

[3] *REMCOM Inc.* , State College, PA 16801.

[4] *"Electronic imaging: Board of Regents,"* National Institutes of Health, National Library of Medicine (U.S.) Board of Regents, Bethesda, MD, Rep. NIH 90-2197, 1990.

[5] Z. P. Liao, H. L. Wong, B. P. Yang and Y. F. Yuan, "A transmitting boundary for transient wave analysis," *Scientia Sinica (Series A)*, vol. 27, no. 10, pp. 1063–1076, October 1984.

[6] J. -P. Berenger, "Perfectly matched layer for FDTD solution of wave-structure interaction problems," *IEEE Trans. Antennas Propagat.*, vol. 44, pp. 110–117, Jan. 1996.

[7] "Recommendation 70-03 relating to the use of short range devices (SRD)," *Conf. Eur. Postal Telecomm. Admin. (CEPT)*, Tromso, Norway, CEPT/ERC/TR70-03, 1997.

[8] G. Lazzi and O. P. Gandhi, "On modelling and personal dosimetry of cellular telephone helical antennas with FDTD code," *IEEE Trans. Antennas Propagat.*, vol. 46, no. 4, pp. 525-530, April 1998.

[9] W.G. Scanlon and N. E. Evans, "Radiowave propagation from a tissue-implanted source at 418 MHz and 916.5 MHz," *IEEE Trans. Biomed. Eng.*, vol.BME-47, no. 4, pp 527–534, April 2000.